Chapter III

Results

Physicochemical properties of DFO in an aqueous solution

Desferroxamine (DFO) is an antidote to iron poisoning (for chemical structure see Figure 1.1). In a N_2-saturated atmospheric aqueous solution, 1 μM DFO possesses an absorption spectrum between 190 nm to 250 nm with the maximum absorbance at 195 nm (Figure 3.1). An incremental concentration, solution of DFO possessed lowering light absorption and the maximum absorbance was shifted to the red side. The solution of 100 μM DFO possessed an absorption band ranging from 190 nm to 240 nm with a maximal absorbance at 208 nm. The spectral shape and lowering in light absorption efficiency of DFO when increasing in its concentration signified that in an aqueous solution, even at low concentration the DFO would be found in aggregate form.

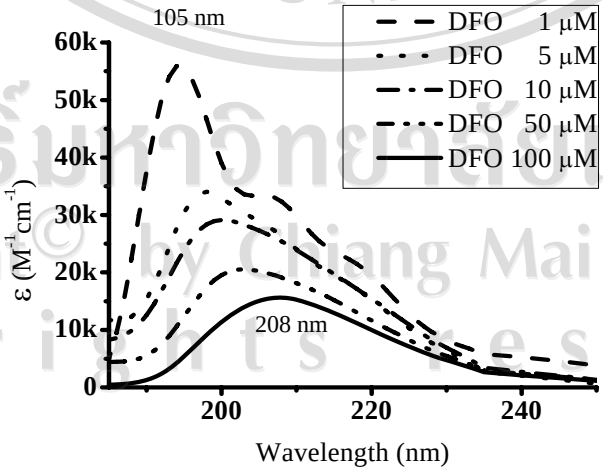

Figure 3.1 Absorption spectra of DFO. An indicated final concentration of DFO was obtained by dissolving in 0.1 mM NaCl , pH 5.6 at 25 ºC.

Potentiometric Titration

DFO can undergo ionization in physiological solutions as indicated in figure 3.2. The pKa values determined by potentiometric titration are 7.23, 7.64, 8.3 and 8.6.

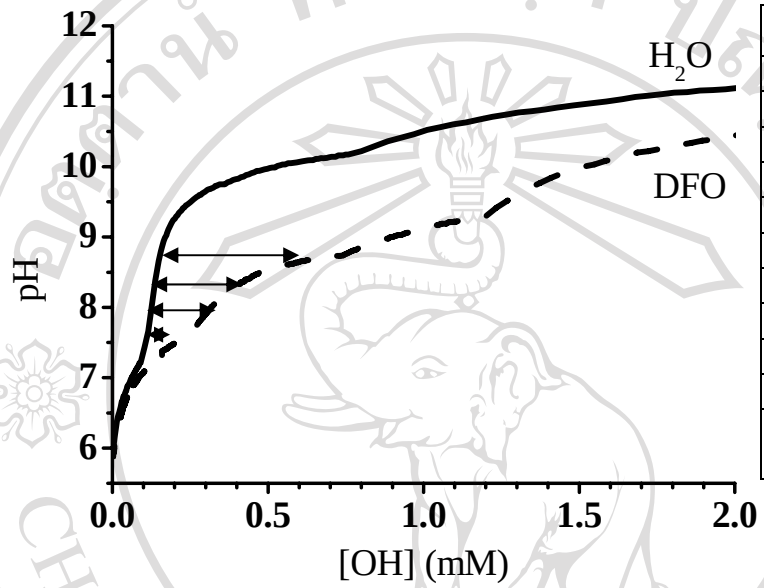

pH	[H+] release form DFO (mM)
6	0.0000
6.5	0.0085
6.8	0.0127
7	0.0223
7.2	0.0430
7.4	0.0664
7.6	0.1310
7.8	0.1605
8	0.1905
8.2	0.2300
8.4	0.2978
8.6	0.3253

Figure 3.2 Variation of pH as a function of NaOH concentration. DFO (0.1 mM) was dissolved in 0.1 mM NaCl , pH 5.6 at 25 ºC. A successive addition of stock solution of 0.01 M or 0.1 M NaOH yielded an increase in pH value.

Complexation of DFO-ferric ion

Deionized double distilled water with $N_{2(g)}$ saturated atmosphere was used as the solvent for reaction of DFO-ferric ion. The spectrum of ferric ion alone, DFO alone and the mixture of 1:1 DFO to ferric ion was shown in Figure 3.3. Initially, DFO solution was colorless and ferric ion solution was pale yellow. And immediately after addition of ferric ion into the DFO solution, the color of the mixture solution

immediately changed to reddish orange. The mixture solution possessed a new absorption band ranging from 300 nm to 600 nm with the maximum absorbance at 427 nm. The reaction was done within 1 minute and the absorbance at 427 nm was stable for at least 24 h.

Spectrophotometric titration of DFO by ferric ion

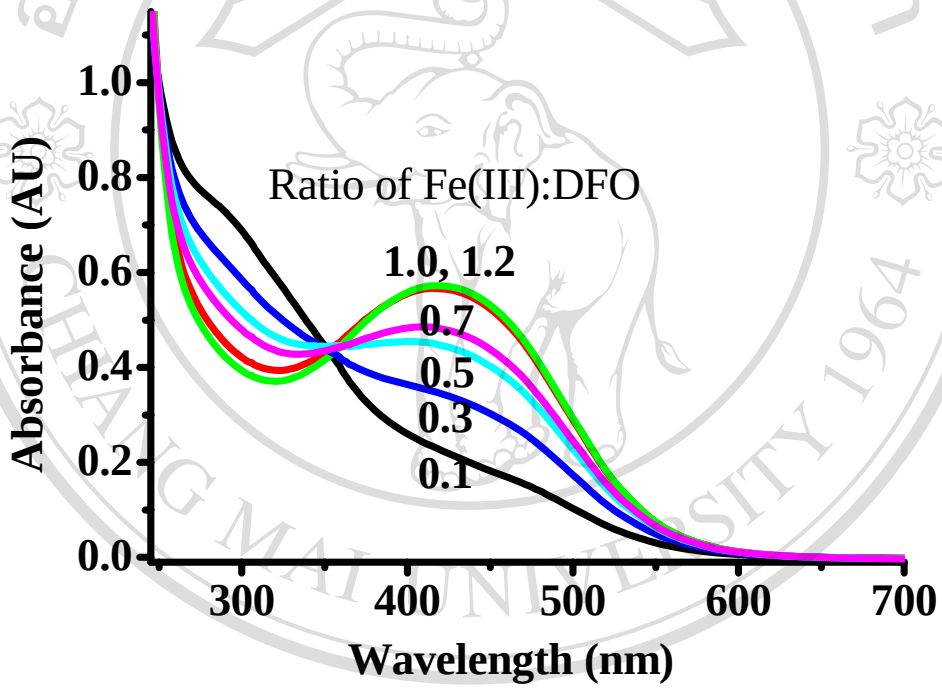

Figure 3.3. Absorption spectra of reaction products of Fe^{3+}-DFO. The initial concentration of DFO was $5x10^{-4}$ M and the final concentration of Fe^{3+} was variable as indicated in the Figure. The reactions were performed in 0.1 M Na^{+}, pH 7.4 at 25ºC.

For the study of the complexation, two series of experiments were performed. In one series, the concentration of DFO was constant to 5 x 10^{-4} M while the

concentration of Fe^{3+} was variable. However, in the other, the Fe^{3+} was constant to 5 x 10^{-4} M and the concentration of DFO was variable.

The spectra of the mixture solutions were recorded at 5 minutes after mixing the two reagents. The typical results of the complexation of Fe^{3+}-DFO were indicated in Figure 3.3. The absorbance at 427 nm increased when the ratio of DFO to Fe^{3+} increased, then reached a pseudo-plateau when the ratio was equal to 1:1 (Figure 3.4). This signified that the complexation was done with stoichiometry of one mole of DFO to one mole of Fe^{3+}. The absorbance at 427 nm of the complex of 1:1 DFO to Fe^{3+} was linear proportion to the concentration of DFO or Fe^{3+}. This signified the characteristic light absorption of the complex. The molar extinction coefficient (ε) at 427 nm was equal to 1607 M^{-1} cm^{-1} (Figure 3.5).

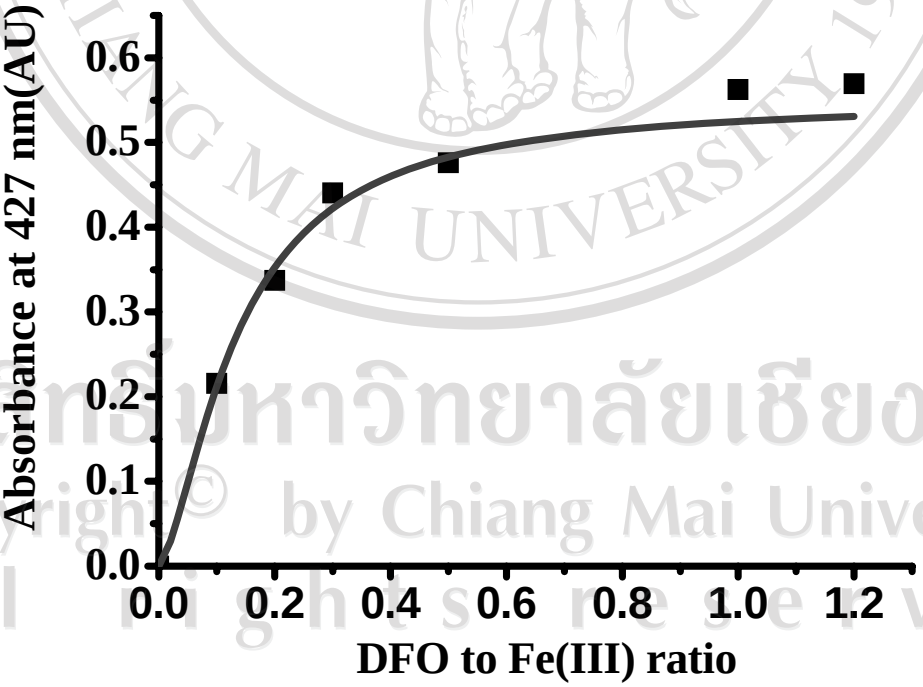

Figure 3.4. Variation of absorbance at 427 nm as a function of the ratio of Fe^{3+} to DFO. These results obtained from Figure 3.3.

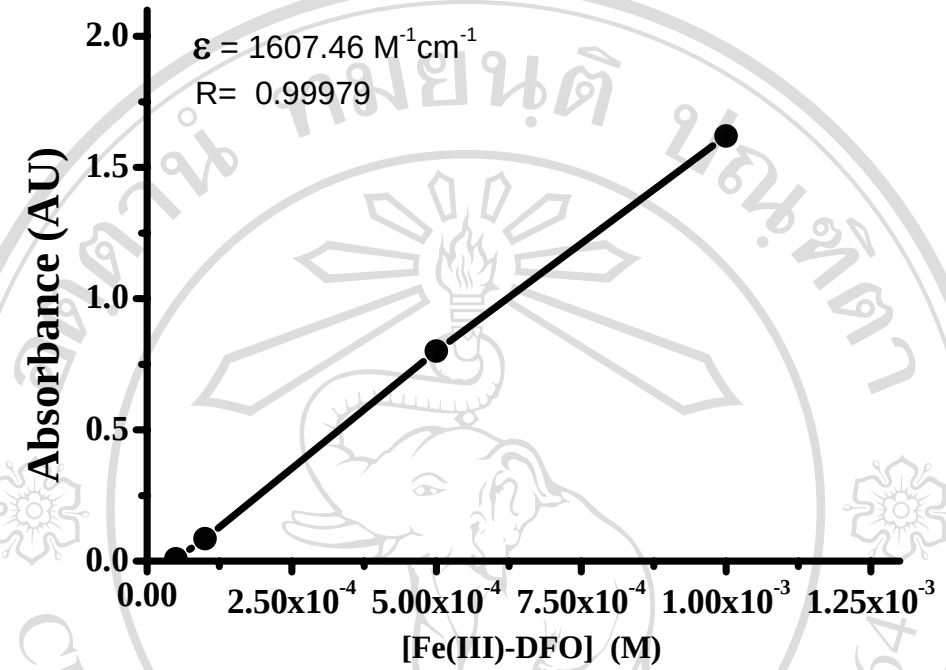

Figure 3.5 Variation of absorbance at 427 nm as a function of concentration of Fe^{3+}or DFO. The initial $[Fe^{3+}]$ = [DFO] varied from 10^{-6} to 10^{-3} M.

Spectrophotometric and potentiometric titration of Fe^{3+}-DFO complex

For determining the stability and ionization constants of Fe^{3+}-DFO, the two series of experiments were performed. First, the initial [DFO] = $[Fe^{3+}]$ = 5 x 10^{-4} M was vigorously mixed for 5 minutes and the pH of solution was adjusted by using 0.01 M HCL or 0.01 M NaOH yielding a pH varied from 3 to 9. The absorption spectra of the solutions at each pH were recorded as indicated in (Figure 3.6). The light absorption of the Fe^{3+}-DFO at pH 7 to 8.4 was almost the same; an absorption band from 300 to 600 nm with the maximum absorbance at 427 nm. The maximum absorbance wavelength was shifted to the red side in an acidic solution such as at pH

levels 5 and 3 (Figure 3.6). This signified that the complex was stable in an aqueous solution at pH 7 through to 8.4. For the second series of experiments, the initial [DFO] = [Fe^{3+}] = 5 x 10^{-4} M was vigorously mixed for 5 minutes then the solution was titrated using 0.01 or 0.1 M NaOH (Figured 3.7). The first ionization of complex was determined and the ionized rate constant (pKa) was equal to 7.2.

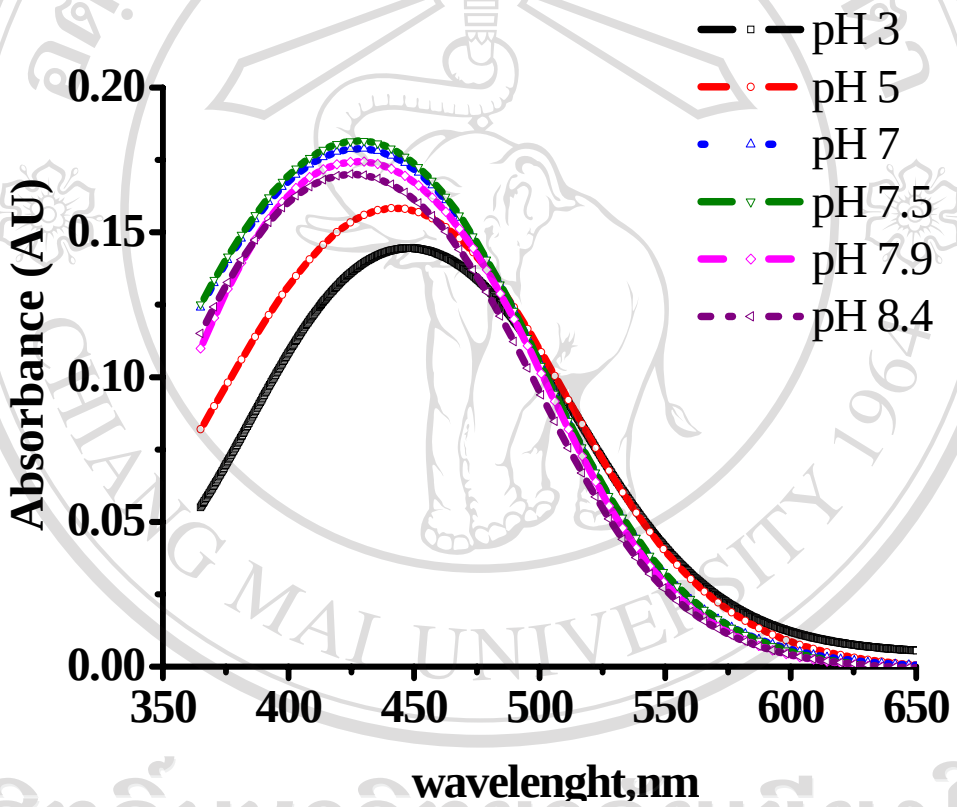

Figure 3.6 Absorption spectra of DFO-Fe^{3+} in solution at indicated pH value. The initial [Fe^{3+}] = [DFO] = 2 x 10^{-4} M.

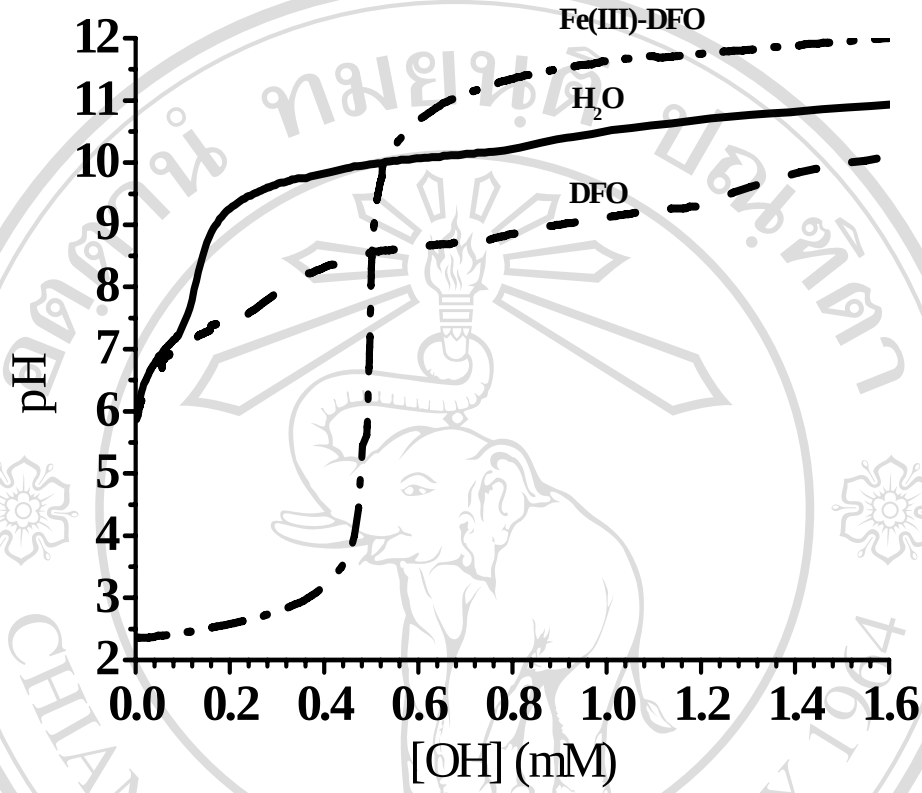

Figure 3.7 Variation of pH as a function of NaOH concentration. The initial [DFO] = $[Fe^{3+}] = 5x10^{-4}$ M, the reaction was performed in 0.1 M Na^{+}, pH 7.4 at 25ºC.

Measurement of T1 relaxation time and relaxivity of Fe(III)-DFO complex

This study proposed to synthesize a ferromagnetic-complex which is intended to be used as a probe for molecular imaging applications, particularly for MR-imaging. For these purposes, the magnetic susceptability of the complex was investigated. T1-weighted images of phantoms were created by using T1w- spin echo mode which was based on the similar principle of an inversion recovery pulse sequence by fixing a TE constant at 15 ms, flip angle at 90º and varied TR from 100

to 6000 ms (Figure 3.8). The intensity of T1 signals were increased and then reached a pseudo plateau at TR equal to 4000 ms for all conditions of experiments including 3.7% agarose gel, RPMI 1640 culture medium and distilled water. The data were quantitatively analyzed by using Block's equation: $M_y = M_z(1 - e^{-(TR/T1)})$. It was reasonable to replace M_y and M_z by I and I_0, respectively. The T1 relaxation time of 3.7% agarose gel, RPMI 1640 culture medium and distilled water were 2381 ms, 3290 ms and 3947 ms, respectively. In the presence of Fe^{3+}-DFO, the T1 relaxation signals increased rapidly with increments of TR time compared with the previous series of experiments without Fe^{3+}-DFO and were also obviously dependent on Fe^{3+}-DFO concentration (Figure 3.9). The T1 relaxation time of protons in the presence of various Fe^{3+}-DFO concentrations was quantitatively determined using the expression of $I = I_0(1 - e^{(TR/T1)})$. The T1 relaxation times of experimental systems in the presence of variable Fe^{3+}-DFO concentration were reported in Figure 3.10.

The relaxivity value or $\left(\frac{1}{T1}\right)$ was plotted as a function of Fe^{3+}-DFO concentration (Figure 3.11) and the data were fitted using linear at least square fit (r^2= 0.999). The Fe^{3+}-DFO relaxivity was determined in the three conditions such as 3.7% agarose gel, RPMI 1640 culture medium and distilled water and almost the same, being equal to 0.0105 ± 0.004 $mM^{-1}.s^{-1}$.

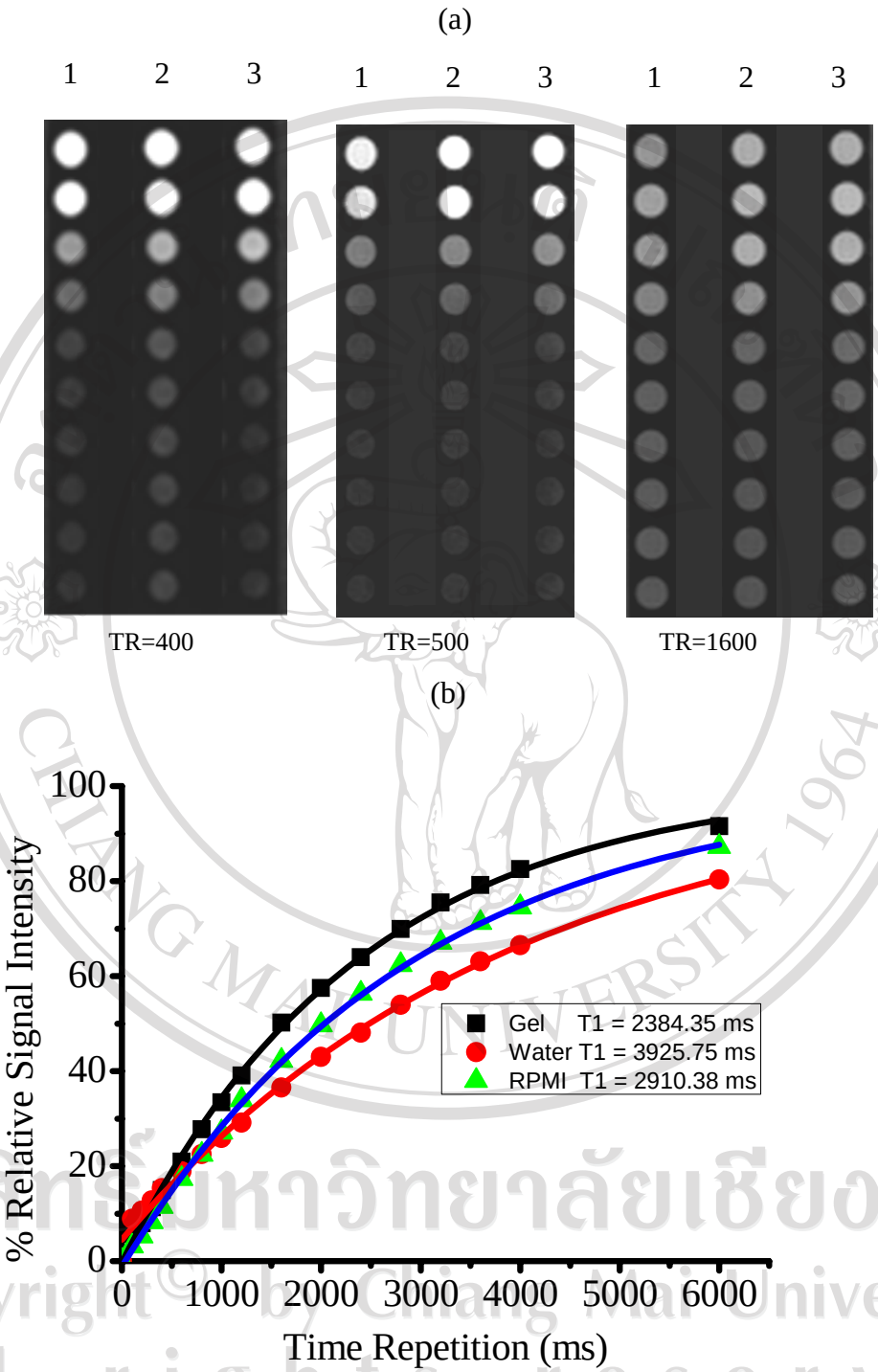

Figure 3.8 T1 weighted images of 3.7% agarose gel, RPMI 1640 culture medium and water phantoms (a) and their relative signal intensity as a function of time repetition. (1 = agarose gel, 2= water, 3=RPMI1640).

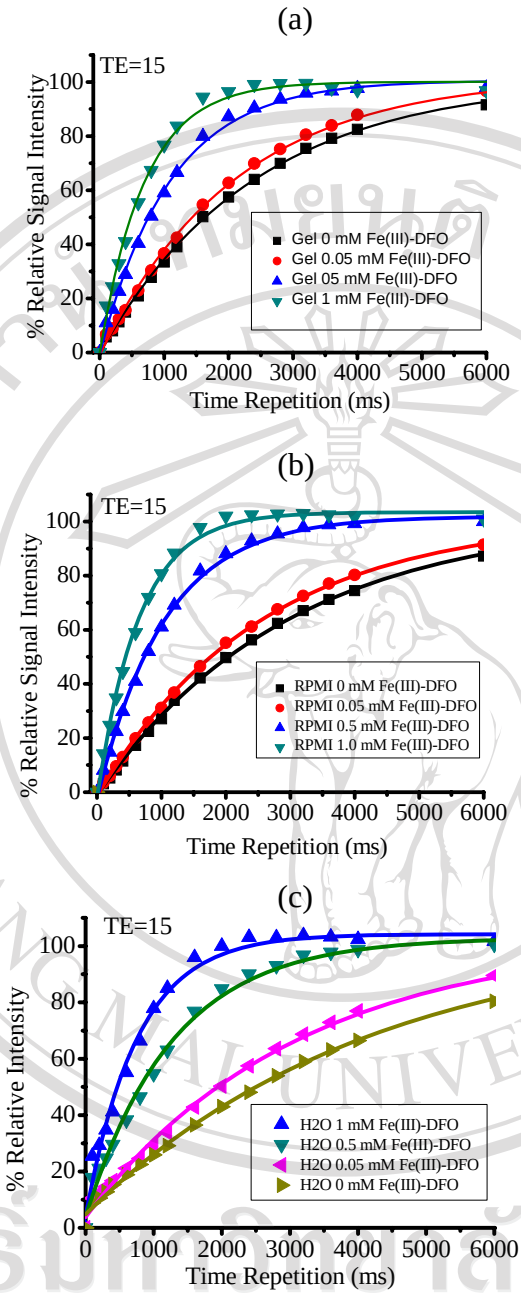

Figure 3.9 Variation of T1 signal intensity measured using (a) 3.7% agarose gel, (b) RPMI 1640 culture medium and (c) distilled water in the presence of indicated Fe(III)-DFO concentration.

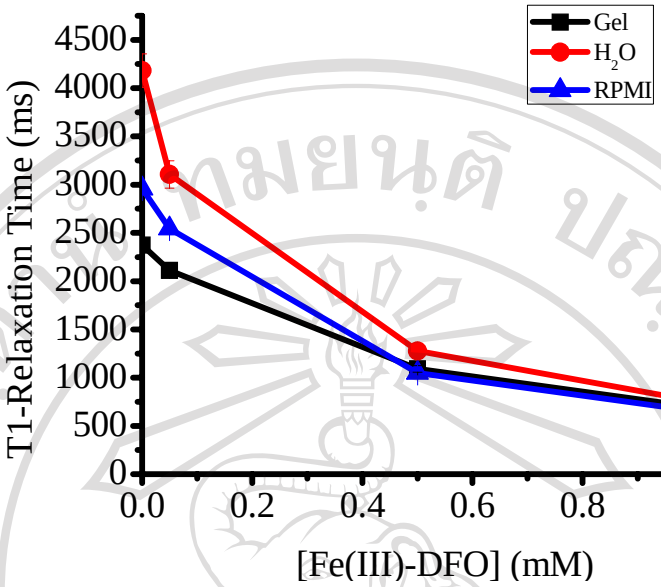

Figure 3.10 Variation of T1 relaxation time as a function of Fe^{3+}-DFO concentration.

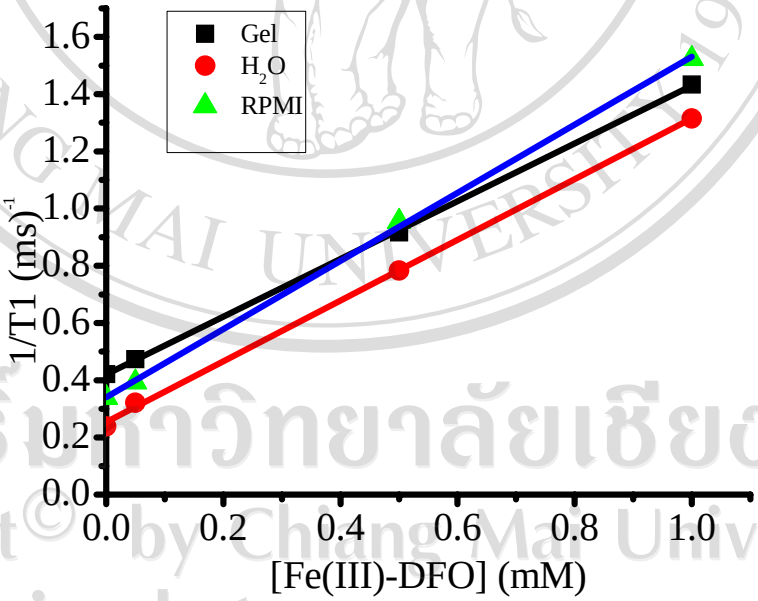

Figure 3.11 The relaxivity value was plotted as a function of Fe^{3+}-DFO concentration.

Measurement of T2 relaxation time and relaxivity of Fe(III)-DFO complex

T2-wieghted images of phantoms were created by using T2w- turbo spin echo mode by fixing a TR constant at 4000 ms, flip angle at 90º and varied TE from 60 to 1000 ms (Figure 3.12).

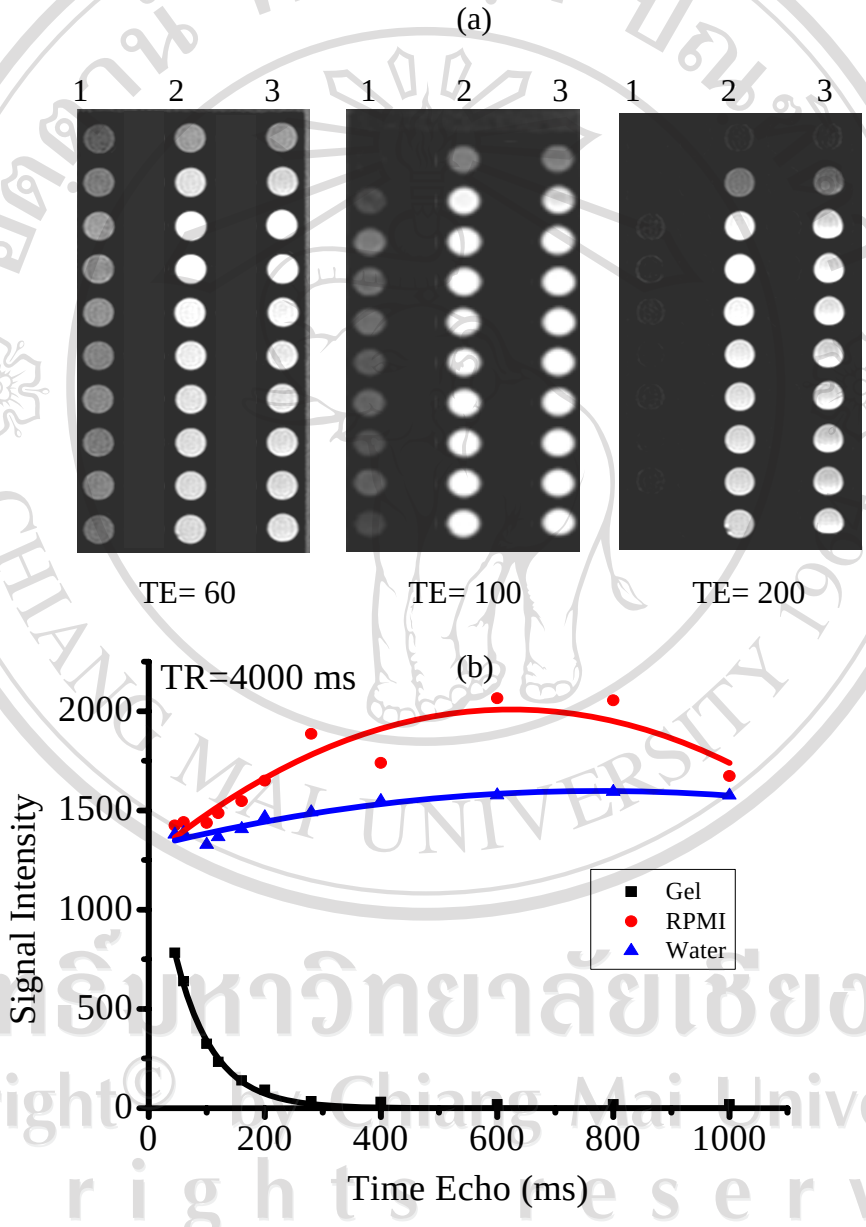

Figure 3.12 T2 wieghted images of 3.7% agarose gel, RPMI 1640 culture medium and water phantoms (a) and their relative signal intensity as a function of time echo. (1 = agarose gel, 2= water, 3=RPMI1640).

It was verified that the T2 signal intensity was almost the same when the similar conditions of experiments were performed by fixing TR constant at 1000 ms. It should be noted that the T2 relaxation time cannot be determined using our conditions of the experiments except for 3.7% agarose gel (Figure 3.13).

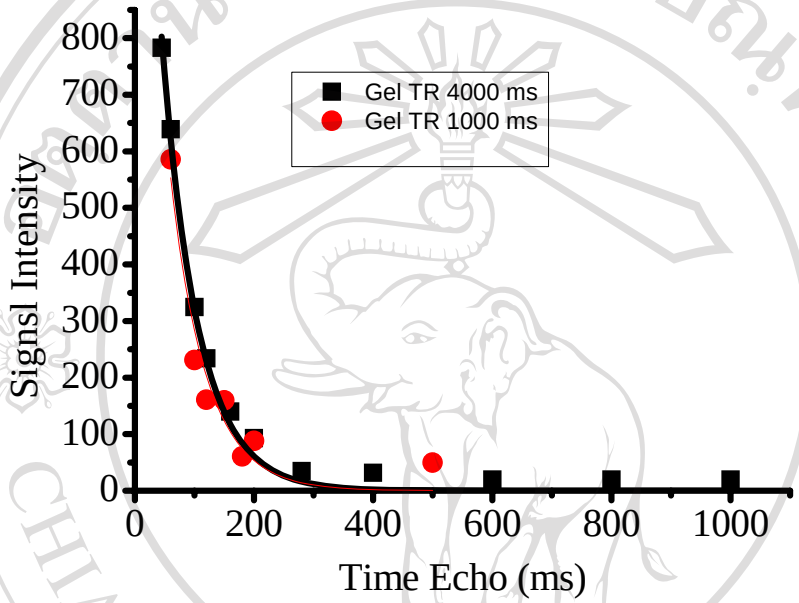

Figure 3.13 T2 wieghted images of 3.7% agarose gel phantoms and their relative signal intensity as a function of time echo on TR dependent of 1000 and 4000 ms.

The T2 signals of gel phase were quantitatively analyzed using Block's equation: $I = I_0 e^{-(TE/T2)}$ and the T2 relaxation time of 3.7% agarose gel was 70 ± 5 ms. Fe^{3+}-DFO complex enhanced a shortened T2 relaxation time of our systems as time echo and in concentration dependent manner (Figure 3.14 and 3.15).

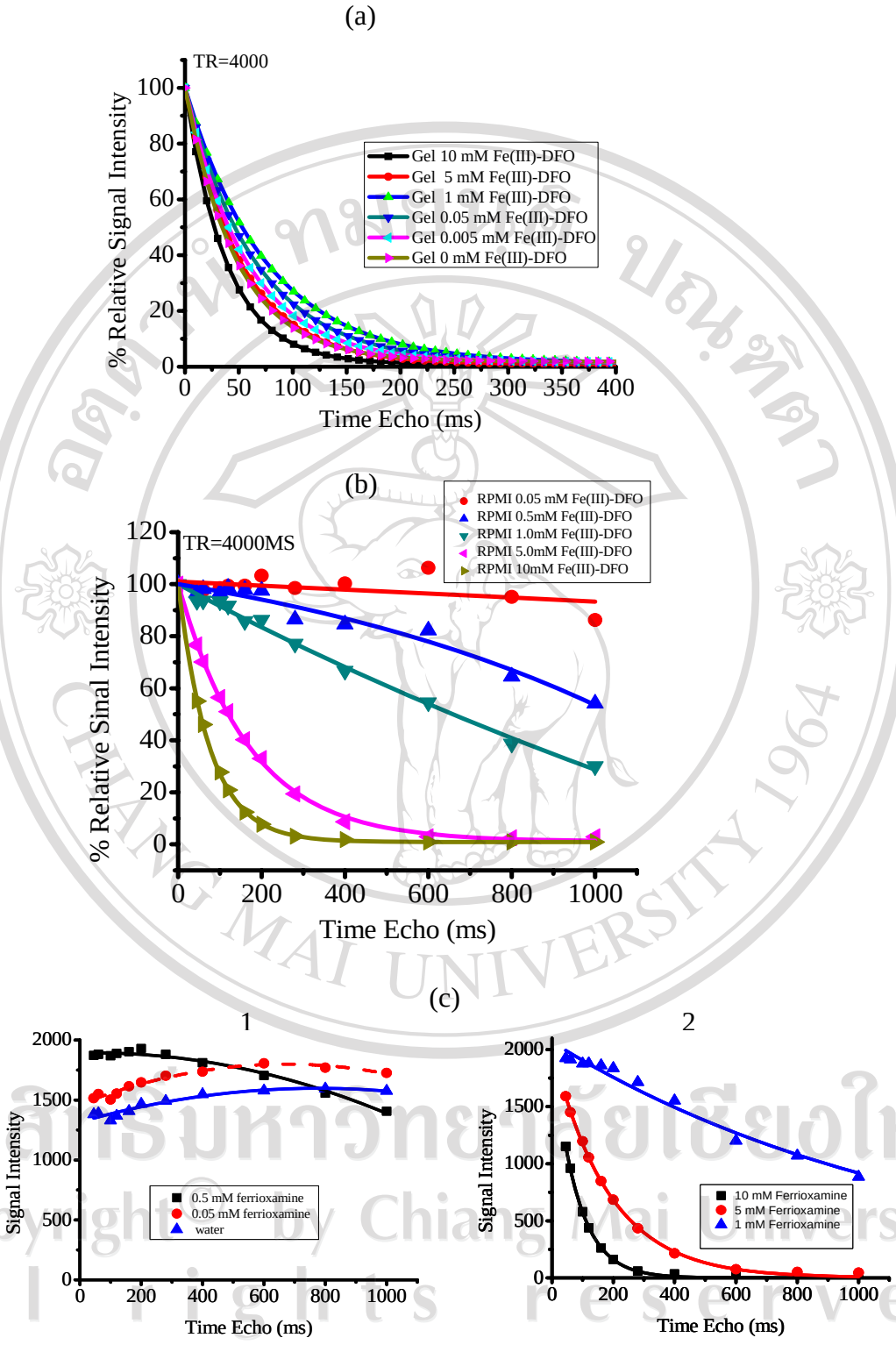

Figure 3.14 Variation of T2 signal intensity measure using (a) 3.7% agarose gel, (b) RPMI 1640 culture medium and (c) distilled water in the presence of indicated Fe^{3+}-DFO concentration.

It was observed that in distilled water (Figure 3.14c), 0.05 mM Fe^{3+} did not affect the T2 relaxation behavior of protons in liquid phase. However, at higher concentrations, such as at 0.5 and 1 mM of the complex affected the T2 relaxation which could easily be determined with longer TE (more than 400 ms for 0.5 mM and 250 ms for 1 mM). The similar results were obtained in RPMI 1640 culture medium (Figure 3.14b). Figure 3.15 and 3.16 showed the influence of Fe^{3+}-DFO complex on T2 relaxation in 3.7% agarose gel. The relaxivity of Fe^{3+}-DFO complex was 1.17± 0.2 $nM^{-1}.s^{-1}$ in 3.7% agarose gel, 1.34 ± 0.2 $nM^{-1}.s^{-1}$ in RPMI 1640 culture medium and 1.45± 0.2 $nM^{-1}.s^{-1}$ in water.

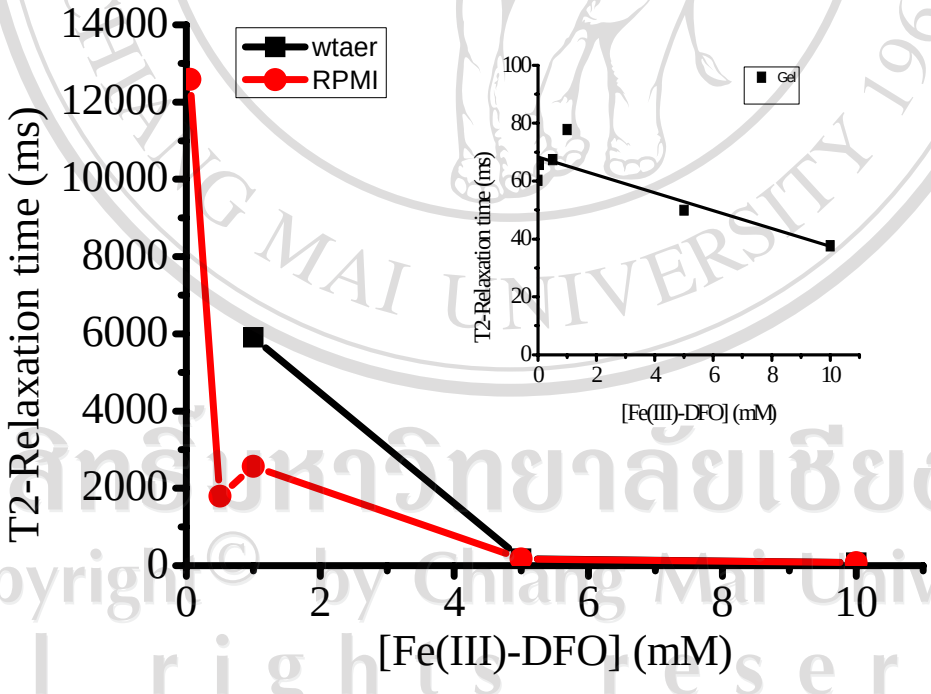

Figure 3.15 Variation of T2 relaxation time as a function of Fe^{3+}-DFO concentration

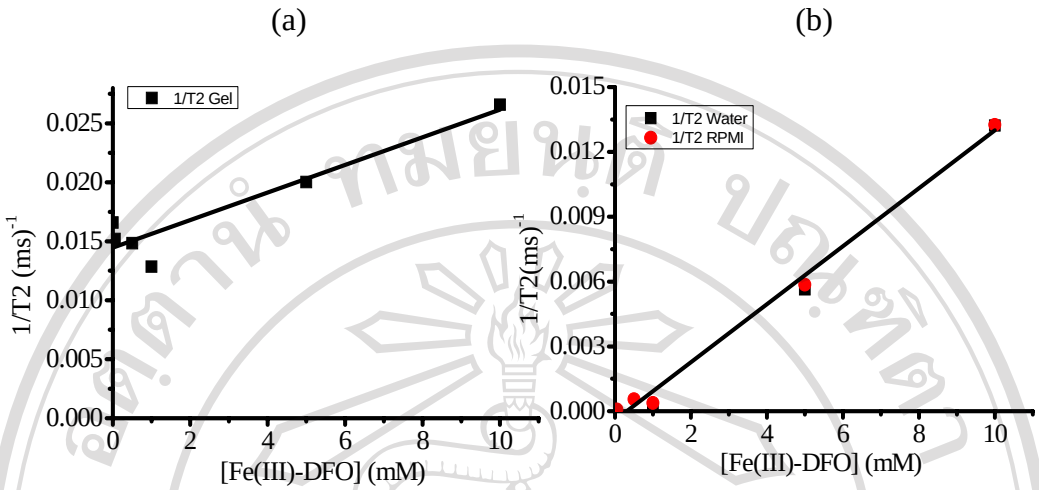

Figure 3.16 The relaxivity value was plotted as a function of Fe^{3+}-DFO concentration.

Bio-distribution in Wistra rats

T1- and T2-weighted images of Wistra rats before and after injection of Fe(III)-DFO complex compared with Gd-DTPA were indicated in Figure 3.17 and 3.18. The results show that Fe(III)-DFO complex enhanced tissue contrast in both T1 and T2 images compared with pre-contrast. T1- and T2-weighted images also demonstrated that Fe(III)-DFO complex provided information of both tissue and blood pool system while Gd-DTPA was found only in blood pool system. The distribution of Fe(III)-complex was clearly demonstrated by using T1-fat suppression and MIP reconstruction technique (Figure 3.19). The signal intensity of various organs as function of time after injection was measured using ROI technique (Figure 3.20).

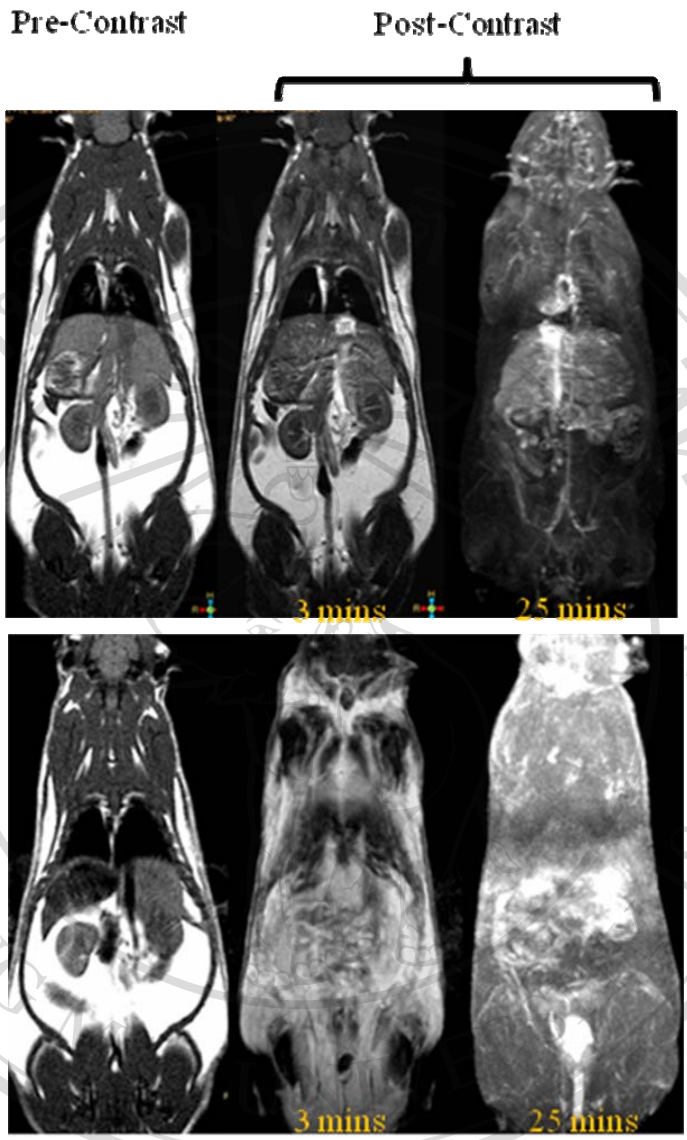

Figure 3.17 T1W-images of Wistra rats pre- and post administrated of Fe(III)-DFO (upper panel) and of Gd-DTPA (lower panel).

All of the images were obtained with head coils. The three-dimensional-spin echo technique (T1W-SE, TR/TE, 15/550 ms; flip angle, 90°) with chemical fat-suppression was used for all rats. The images were acquired before injection of the contrast agents and at 3 and 30 min post-injection. The coronal images were reconstructed with 1.0 mm section thickness and 0.5 mm overlap. The FOV was 279 mm.

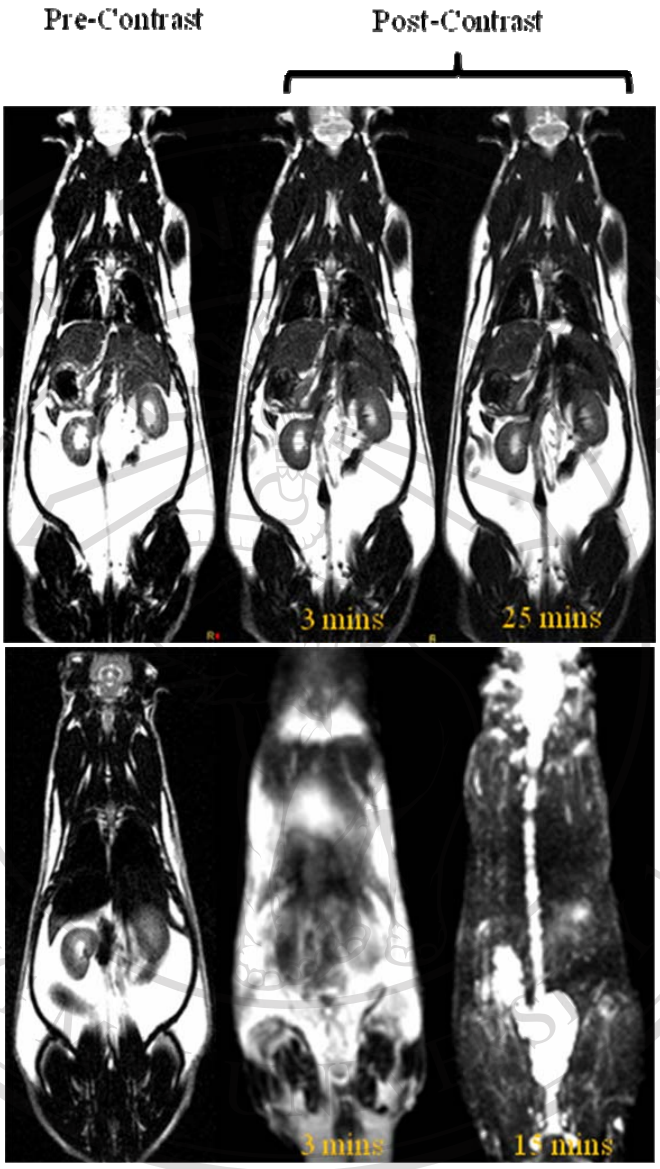

Figure 3.18 T2W-images of Wistra rats pre- and post administrated of Fe(III)-DFO (upper panel) and of Gd-DTPA (lower panel).

All of the images were obtained with head coils. The three-dimensional-turbo spin echo technique (T2W-TSE; TR/TE, 120/2910; flip angle, 90°) with chemical fat-suppression was used for all rats. The images were acquired at indicated time post-injection. The coronal images were reconstructed with 1.0 mm section thickness and 0.5 mm overlap. The FOV was 279 mm.

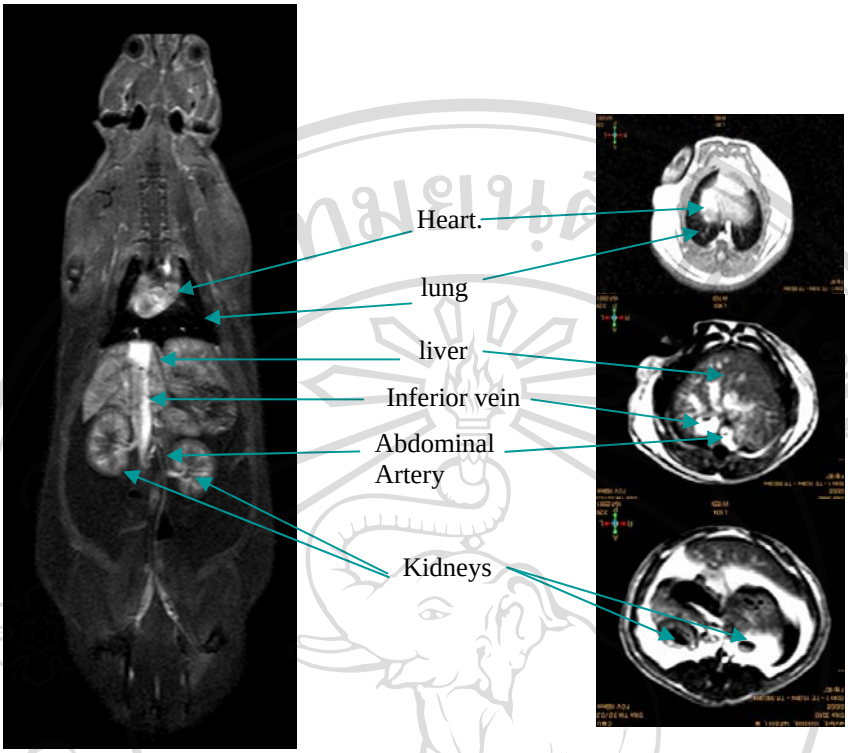

Figure 3.19 T1 fat suppression coronal and cross section image of Wistar rat with anatomy labels.

All T1 fat suppression images were obtained with head coils. The three-dimensional-spin echo technique (T1W-SE, TR/TE, 15/550 ms; flip angle, 90°) with chemical fat-suppression was used for all rats. The images were acquired before injection of the contrast agents and at both 3 and 30 min post-injection. The coronal images were reconstructed with 1.0 mm section thickness and 0.5 mm overlap. The FOV was 279 mm.

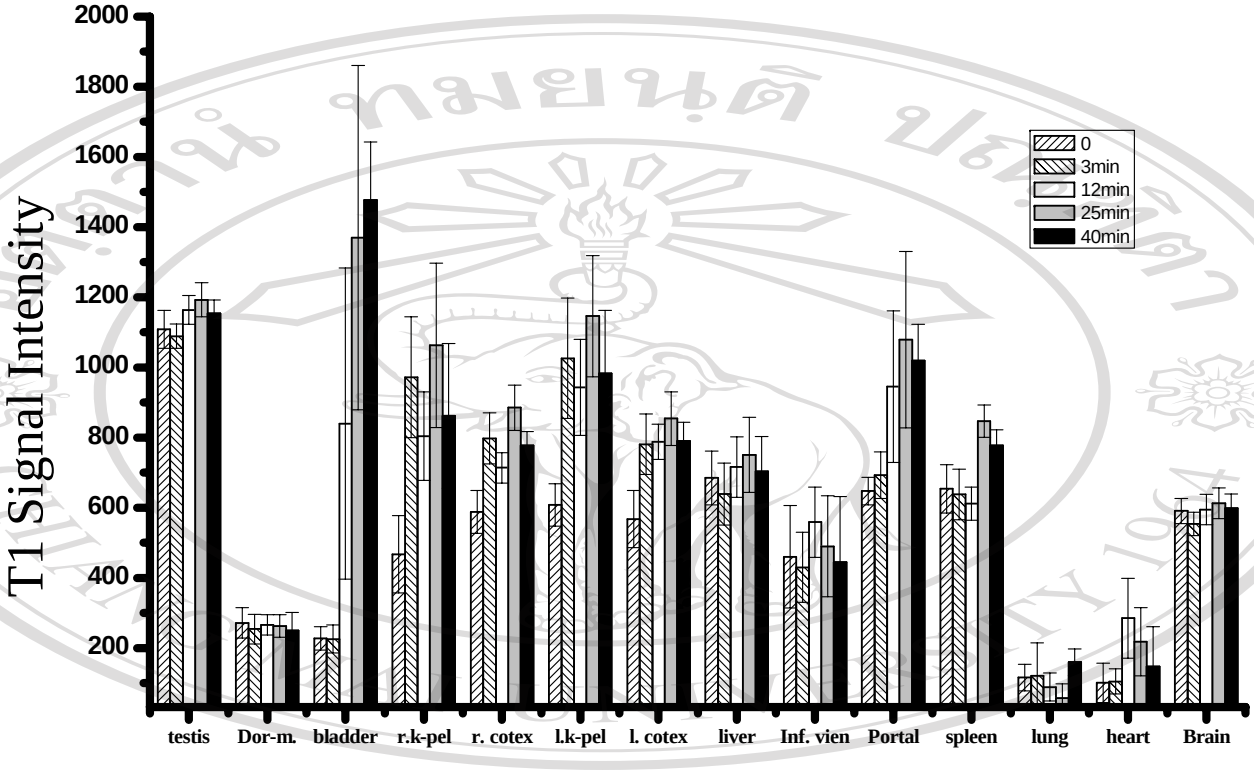

Figure 3.20 Variation of T1 signal intensity as a function of time. The T1 signal intensity was measured from T1W- images obtained by using ROI technique